J. Opt. A: Pure Appl. Opt. **2** (2000) 294–298. Printed in the UK PII: S1464-4258(00)10390-3

Longitudinal extra torque in liquid crystals due to the optical beam shape

L Marrucci, B Piccirillo, F Vetrano and E Santamato

Università di Napoli 'Federico II' and Istituto Nazionale per la Fisica della Materia, Dipartimento di Scienze Fisiche, Monte S Angelo, via Cintia, 80126, Napoli, Italy

Received 14 December 1999, in final form 7 March 2000

Abstract. Optical reorientation in nematic liquid crystals turns out to depend not only on the intensity and polarization of the pumping laser beam, but also on the shape of the transverse cross-section. A longitudinal extra torque acting on the molecular director appears whenever the beam cross-section shape breaks the system cylindrical symmetry.

Keywords: Nematic liquid crystals, homeotropical alignment, nonlinear optics, molecular reorientation

1. Introduction

Most of the physics ruling over the nonlinear optics of liquid crystals is already understood [1–3]. The reorientation process of the molecular director is usually induced by a polarized laser beam of suitable intensity, whose electric field strongly interacts with the director itself. The well known optical Fréedericksz transition (OFT) [4, 5] and many other complex effects such as self-induced stimulated light scattering [6–8], intrinsic optical bistability [9], laser-induced chaotic optical oscillations [10–14], etc, are based on such a mechanism. In this work we explored the possibility of controlling the molecular reorientation by means of another parameter of the laser beam, namely its cross-sectional shape. To this purpose, the occurrence of a longitudinal extra torque due to a beam cross-section shape breaking the system cylindrical symmetry has been experimentally probed.

At first, to single out the beam-shape effects, an unpolarized elliptically shaped laser beam was used. With unpolarized light all contributions to the longitudinal torque arising from the light polarization vanish; therefore, all molecular reorientations around the beam axis are driven by the 'beam-shape torque'. Then, in order to evaluate the importance of this beam-shape torque with respect to the polarization torque, polarized light was also used.

A similar beam-shape torque turns out to play a crucial role in frequently occurring situations such as in experiments made at a very large oblique incidence angle or, even more, in strongly asymmetric geometries as in planar optical waveguides.

In our experiments, to obtain an elliptical beam cross-section at the sample position, a spherical lens and a cylindrical lens were put in cascade so as to have their focal points superimposed (see figure 1). The beam-shape torque arises along the propagation (longitudinal) direction of the beam and tends to rotate the molecules towards the major axis of the elliptical beam profile. Its strength vanishes for circular cross-section and increases for rising-beam eccentricity. Finally, irradiating the sample by means of a laser beam linearly polarized at 45° with respect to the major axis of the cross-section ellipse, a competition between the beam-shape torque and the polarization torque was observed, showing that the two torques can be of comparable magnitude.

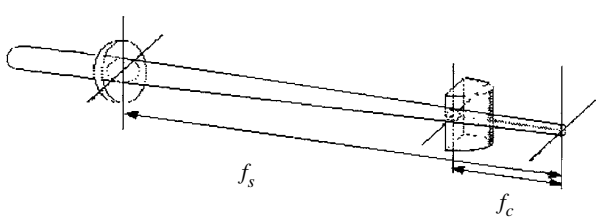

Figure 1. The system made of a spherical and a cylindrical lens in near confocal configuration adopted in our experiment to obtain an elliptical beam cross-section at the sample position.

2. Molecular reorientation driven by the laser beam shape

For the time being, the full complexity of the beam-shape-induced reorientation is still beyond our grasp and a quantitative model is missing. Nevertheless, a qualitative explanation of the effect may be easily produced.

Consider a homeotropically aligned nematic liquid crystal (NLC) film irradiated by an elliptically shaped unpolarized beam at normal incidence. Initially, the nematic molecular director is oriented normal to the film surfaces and parallel to the beam axis z. For sufficiently large light intensity, however, the optical field will reorient the NLC molecules. The new equilibrium state can then be given by

1464-4258/00/040294+05$30.00

specifying the polar angles θ and ϕ of the molecular director, defined in figure 2, as a function of the position inside the sample. This molecular orientation is not uniform because it must vanish outside the beam spot area and in proximity of the film plane boundaries (we are assuming strong NLC anchoring). Usually, however, the angle ϕ defining the transverse direction of the reorientation is approximately uniform, as the boundary conditions do not set any preferred value for it. Therefore, in the following we will suppose that ϕ is uniform in the whole sample. Within this hypothesis, and assuming that the reorientation angle is small ($\theta \ll 1$), the elastic reaction of the nematic is given by the sum of three independent contributions, as shown in figure 3, respectively associated with a splay deformation along the transverse direction of the reorientation (i.e. at angle ϕ), a twist along the orthogonal transverse direction, and a bend along the longitudinal direction z. The longitudinal deformation extends over a fixed length given by the film thickness, while the two transverse deformations are characterized by a length that depends on the beam elliptical spot size and orientation. This fact introduces a coupling between the beam elliptical spot orientation and the nematic reorientation. In particular, if the reorientation takes place along the direction of the ellipse major axis, as in figure 3, the free-energy density is approximately given by

$$F_e \simeq \left(\frac{k_{11}}{a^2} + \frac{k_{22}}{b^2} + \frac{k_{33}}{L^2}\right)\theta^2, \qquad (1)$$

where a and b denote the lengths of the beam ellipse major and minor axes, respectively, L the film thickness, and k_{11}, k_{22}, k_{33} the splay, twist, and bend elastic constant, respectively. On the other hand, if the molecular director reorients along the direction of the ellipse minor axis, F_e is approximately given by

$$F_e \simeq \left(\frac{k_{11}}{b^2} + \frac{k_{22}}{a^2} + \frac{k_{33}}{L^2}\right)\theta^2. \qquad (2)$$

As the splay constant k_{11} is usually larger than the twist constant k_{22}, expression (1) will be smaller than expression (2), and reorientation to the major axis plane turns out to be energetically preferable.

3. The experiment

The experimental set-up is shown in figure 4. The NLC utilized was the commercial mixture E7, produced by Merck, at room temperature. At +20 °C, the E7 mixture is characterized by the ratio $k_{33}/k_{11} = 1.54$. The sample, whose nominal thickness was 50 μm, was pumped by a frequency-doubled Nd:Yag cw laser (wavelength $\lambda = 532$ nm) having a maximum output power of 5 W. The laser beam was sent through a variable attenuator and then through a Pockels cell (PKC) to obtain depolarized light. The PKC fast axis was oriented at 45° with respect to the laser polarization plane and the cell was driven by a saw-tooth signal at λ-amplitude and a frequency of 200 Hz. This produced a 200 Hz periodic modulation of the light polarization through the sequence of states shown in figure 5. The time-averaged Jones matrix $J_{ij} = \langle E_i E_j^* \rangle$ of this varying polarization state is equal to the

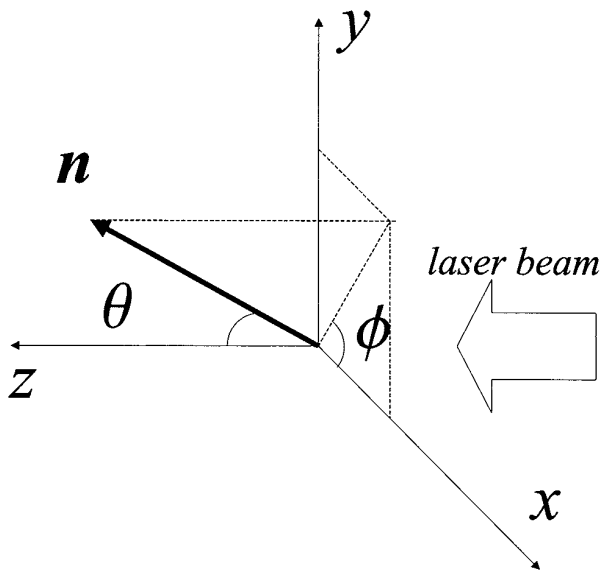

Figure 2. Geometry of the system and polar angles of the molecular director.

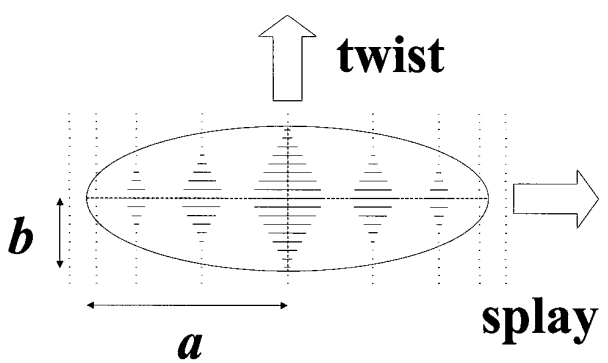

Figure 3. Nematic deformation induced by an elliptical laser beam, for the case in which the reorientation is parallel to the ellipse major axis.

unit matrix (or, equivalently, all its average Stokes' parameters vanish) as for fully unpolarized light. In our case, the NLC orientational dynamics is much slower than the modulation period (∼1 s), so that it will only actually respond to the time-averaged Jones matrix (or Stokes' parameters) of the polarization. Therefore, the laser beam emerging from the PKC is, for our purposes, completely equivalent to unpolarized light. By means of a polarimeter, we verified that the three Stokes' parameters did average to zero on the NLC response-time scale. The measurements requiring linearly polarized light were instead made without the PKC.

The spherical lens (SL; $f_s = 500$ mm) and the cylindrical lens (CL; $f_c = 15$ mm), assembled in the nearly confocal configuration (see figure 1), were used to obtain an elliptical spot on the sample. The major-to-minor axis ratio e of the beam spot size on the sample was changed by moving the NLC film across the focal zone of the two lenses. In this way e could be changed from 1 to about 5. In practice, the vertical dimension of the laser spot was kept fixed at about 75 μm (half-width at $1/e^2$ intensity), while the other dimension ranged from 15 to 75 μm.

We probed the NLC molecular reorientation by looking

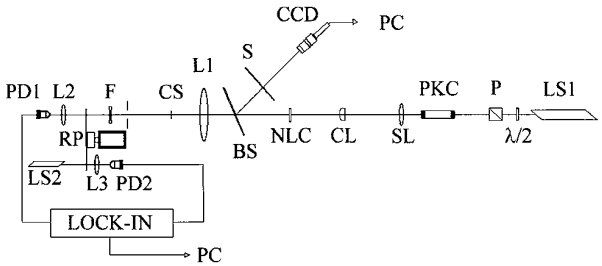

Figure 4. Our experimental apparatus. LS1, LS2, laser sources; P, polarizer; PKC, Pockels cell; SL, spherical lens; CL, cylindrical lens; NLC, liquid crystal sample; S, screen; BS, beam splitter; CS, circular spot; F, neutral filter; L1, L2, L3, lenses; PD1, PD2, photodiodes; RP, rotating polarizer; PC, personal computer.

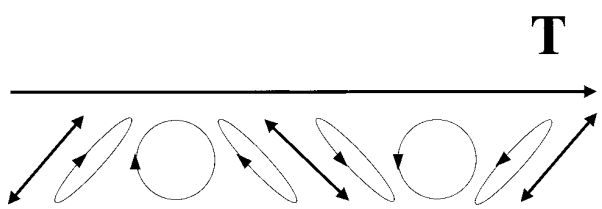

Figure 5. Polarization state sequence in our artificially depolarized light.

at the characteristic far-field self-diffraction ring pattern [4,5] generated by the light after passing through the sample. In particular, we measured the angular divergence and the average polarization of the ring pattern by means of the following optical system. Beyond the NLC sample, a beam splitter (BS2) divided the emerging light into two parts. The reflected light was sent onto a screen (S), where the ring pattern was recorded by a CCD camera. From the acquired pattern, the angular aperture (Θ) of the outermost ring could be determined. More precisely we recorded Θ of the outermost ring along a fixed direction on the screen, as the diffraction pattern generated by an elliptical beam does not have exact circular symmetry. The light transmitted by the beam splitter (BS2) was first deprived of its central zone by means of a circular stop (CS), to get rid of undiffracted light. Then it was collected by a large aperture (15 cm diameter) lens (L1; $f_1 = 500$ mm), analysed by a linear polarizer (RP) rotating at about $\nu = 50$ Hz frequency, and finally focused by a lens (L2) on a photodiode (PD1). The output of the photodiode was then sent into the signal channel of a lock-in amplifier. A linearly polarized red diode laser (LS2) passed through the same rotating polarizer (RP) and was collected by a lens (L3) into a second photodiode (PD2) to provide the reference signal to the lock-in. The phase difference $\Delta\psi$ between signal and reference was determined by the lock-in and sent to the PC for storage and real-time visualization, together with Θ.

Let us now assume that the ring pattern is approximately linearly polarized along some angle ϕ_1. The phase $\Delta\psi$ is then simply related to the polarization angle with respect to the reference beam polarization angle ϕ_2. Indeed, the signals $I_1(t)$ and $I_2(t)$ detected by the photodiodes PD1 and PD2 will be modulated by the rotating polarizer as $I_i \propto \cos^2(2\pi\nu t + \phi_i) = \cos(4\pi\nu t + 2\phi_i)/2 + 1/2$. The phase difference between the two signals $I_1(t)$ and $I_2(t)$ will be $2\phi_1 - 2\phi_2 = \Delta\psi$, which then allows us to determine the polarization direction of the diffracted light with respect to the polarization direction of the reference beam.

In general, the precise relationship between the diffraction-pattern features and the molecular director configuration inside the sample is complex. However, if the reorientation is small, i.e. $\theta \ll 1$, and its direction as specified by the angle ϕ is uniform, we may obtain an approximate relationship that is quite simple. First, the diffraction pattern divergence, as specified for example by Θ, is proportional to the birefringence induced by the reorientation and therefore to θ^2 [15]. Second, only the extraordinary wave polarized parallel to the reorientation direction ϕ is actually diffracted because it 'sees' a nonuniform effective refractive index. The ordinary wave, polarized orthogonal to the reorientation plane, sees instead a spatially uniform refractive index and propagates undiffracted through the sample. The diffraction ring pattern will therefore be approximately polarized along the same direction of the director reorientation, specified by the angle ϕ. Hence, we may set $\phi = \Delta\psi/2$, where the angle ϕ is measured set with respect to the polarization direction of the reference beam†. We note that this detection scheme works well only if there is always some amount of extraordinary wave component in the input light, or otherwise the diffraction pattern would have a vanishing intensity. When we used unpolarized input light in our experiment, both ordinary and extraordinary waves were present with equal intensity for any reorientation direction ϕ so that this condition was always satisfied. Alternatively, when we used linearly polarized input light, instead, our apparatus would fail whenever the reorientation was orthogonal to the input polarization. However, this particular configuration cannot be an equilibrium state of our system, as it makes the optical torque vanish so that the deformation is not sustained.

To summarize we may write

$$\Theta \propto \langle\theta^2\rangle, \qquad \Delta\psi \approx 2\phi, \tag{3}$$

where $\langle\cdot\rangle$ denotes here a spatial average across the NLC film. Although these relationships are only approximate and hold true for weak elastic distortion in the NLC, their main feature that Θ and $\Delta\psi$ are related to independent degrees of freedom of the molecular director configuration also remains valid in more general situations. For example, even if there is substantial longitudinal twist in the sample, i.e. $\phi = \phi(z)$, Mauguin's theorem (valid on conditions that are verified in most cases) ensures that the diffraction rings would still be approximately polarized in a direction given by the angle $\phi(z = L)$ at the exit face of the sample [16].

Although our apparatus allowed measurements of the orientational dynamics of the NLC, here we report only steady-state values of the azimuthal angle ϕ as a function of the beam intensity I and spot eccentricity e. The study of the reorientational transient dynamics is deferred to a future work. Moreover, in this paper we focused our attention only on the angle ϕ because it is the orientational degree of freedom affected by longitudinal torques. The director polar tilt θ, experimentally determined from Θ, is only weakly affected by beam-shape effects.

† The main reason why the ring pattern is not exactly linearly polarized is that part of the light diffracted in the middle of the NLC sample must propagate through the sample itself, obliquely with respect to the optical axis, and therefore it becomes elliptically polarized owing to the sample birefringence.

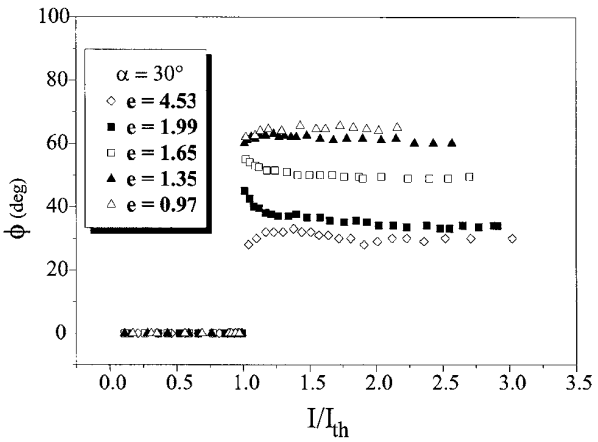

Figure 6. Steady-state value of the director average azimuthal angle ϕ as a function of the reduced laser intensity $I/I_{\rm th}$ for different values of e of the unpolarized beam spot at the sample. The spot ellipse major axis was oriented at $\alpha = 30^\circ$. Below threshold ($I/I_{\rm th} < 1$), the angle ϕ has no physical meaning.

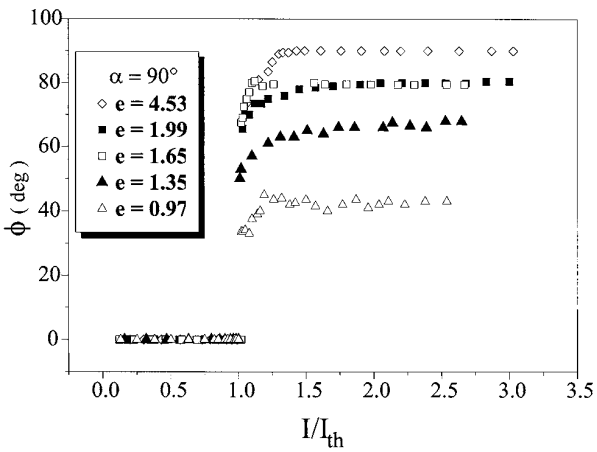

Figure 7. Steady-state value of the director average azimuthal angle ϕ as a function of the reduced laser intensity $I/I_{\rm th}$ for different values of e of the unpolarized beam spot at the sample. The spot ellipse major axis was oriented at $\alpha = 90^\circ$. Below threshold ($I/I_{\rm th} < 1$), the angle ϕ has no physical meaning.

3.1. Measurements with unpolarized light

The steady-state average value of the molecular director angle ϕ was measured for different values of I, e, and orientation of the elliptical spot major axis. To change the orientation of the major axis, specified by the angle α with respect to the horizontal plane, the cylindrical lens was rotated around the beam propagation direction. Data were taken at $\alpha = 0^\circ$, 30°, 60° and 90°. In all cases we found that, for large enough eccentricity ($e \geqslant 2$) and large enough intensity ($I \geqslant 1.3 I_{\rm th}$, where $I_{\rm th}$ is the OFT threshold intensity), the molecular director tends to move towards the plane containing the ellipse major axis, as shown in figures 6 and 7. This demonstrates, on an experimental basis, the existence of the above-mentioned beam-shape extra torque.

For fixed intensity values, as the beam shape becomes more and more circular ($e \to 1$), the steady-state value of ϕ tends towards a well defined but unpredictable value, changing from point to point in the sample. The molecular director was observed behaving likewise even with the beam intensity decreasing towards the OFT threshold for fixed eccentricity values. It is worth noting that, in a NLC film reoriented by unpolarized light, a similar attitude in the steady-state value of ϕ was observed in previous experiments made with a circular laser spot [17, 18]. The unpredictable azimuthal reorientation may be ascribed to small uncontrolled and unavoidable factors breaking the perfect overall cylindrical symmetry of the system *NLC sample + optical field*, such as nonperfect parallelism of the sample walls, residual polarization in the incident light, small deviations from perfect normal incidence, small pre-tilt at the sample surface and so on.

The measured threshold intensity for a circular spot ($e = 1$) was $I_{\rm th} = 7.16$ kW cm^{-2}. As e is increased, the threshold intensity rises slightly.

3.2. Measurements with polarized light

Removing the PKC and properly rotating the cylindrical lens, we pumped the NLC sample by means of a laser beam linearly polarized along a direction making an angle of 45° with respect to the elliptical spot major axis (see figure 8). For large enough laser intensity the steady-state value of ϕ came out to be intermediate between about 0°, at small values of e, and 45° at larger values of e. In other words, a competition between the beam-shape-induced torque and the polarization-induced torque was evident. In this case, the residual torques traceable back to small factors breaking the cylindrical symmetry give way to the stronger polarization torque. Moreover, the beam-shape-induced torque and the polarization-induced torque have comparable strength. Since both torques are roughly proportional to laser intensity, the steady-state value of ϕ is almost independent of the intensity itself. Besides, it seems to depend on the degree of eccentricity of the spot: the higher the parameter e is, the more effectively the director tends to align towards the ellipse major axis plane, as clearly shown in figure 9. For a laser intensity I very close to the threshold, some dependence of ϕ on I was observed. This behaviour finds no simple explanation and it could be possibly ascribed to the poor sensitivity of the experimental apparatus just above the OFT threshold†.

Also in this case, however, the threshold intensity comes out to be almost independent of e and, as expected [17], it reduces to about half of the value for unpolarized light, $I_{\rm th} = 4.18$ kW cm^{-2}.

4. Conclusions

This work demonstrates, on an experimental basis, the occurrence in NLCs of a new optical torque directed along the laser beam and related to the shape of the beam at the sample position. This longitudinal extra torque vanishes in the case of a circularly shaped beam.

The beam-shape torque competes with the usual optical torque due to beam polarization. In order to isolate

† Close to the threshold the accuracy of measurements is reduced because the far-field ring pattern is almost completely intercepted by the circular stop.

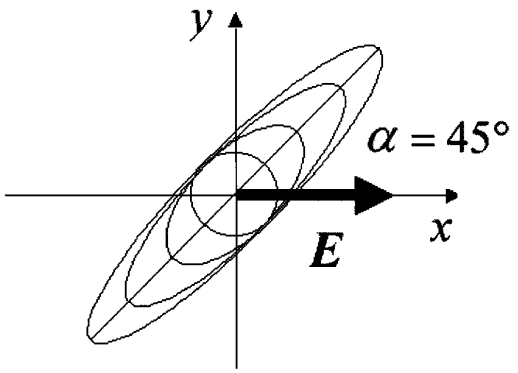

Figure 8. Schematic representation of the mutual orientation of the laser beam polarization and the spot ellipse major axis.

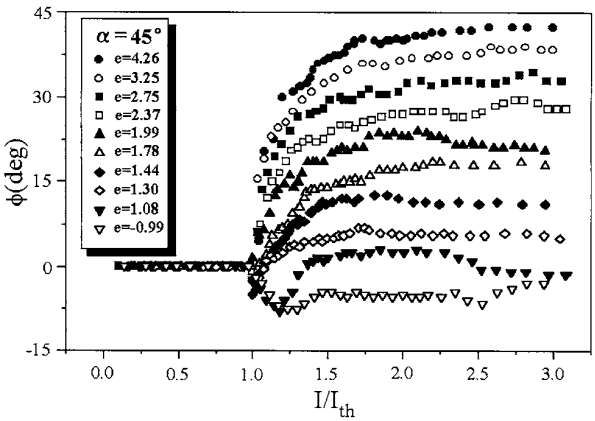

Figure 9. Steady-state value of the director average azimuthal angle ϕ as a function of the reduced laser intensity $I/I_{\rm th}$ for different values of e of the unpolarized beam spot at the sample. The laser beam was linearly polarized in the horizontal plane $\phi = 0$ and the spot major axis was oriented at $\alpha = 45^\circ$ with respect to the same plane.

the beam-shape torque, we used unpolarized light. We observed that, for large enough e, the laser-induced molecular reorientation in the nematic film always occurs in the spot ellipse major axis plane. For low eccentricity values, i.e. $e < 2$, the reorientation plane was governed by minor unavoidable symmetry-breaking imperfections and, hence, it was unpredictable. We repeated our measurements using a laser beam polarized at 45° with respect to the ellipse major axis. In this case, the steady-state reorientation occurs at an intermediate angle between the ellipse major axis and the beam polarization direction, confirming the competition between the beam-shape-induced and polarization-induced torques.

The beam-shape torque should originate ultimately from the lack of cylindrical symmetry in the incident beam, although simple elastic energy considerations suggest that the phenomenon is also related to the anisotropy of the NLC elastic constants. Our measurements are not accurate enough to provide detailed quantitative information about the beam-shape-induced torque, for example concerning how this torque depends on laser intensity and beam eccentricity. Future work is planned in this direction.

Acknowledgments

We thank Istituto Nazionale per la Fisica della Materia (INFM) and Ministero dell'Università e della Ricerca Scientifica e Tecnologica (MURST), Italy, for financial support. BP acknowledges partial financial support from the European Social Fund.

References

[1] Tabiryan N V, Sukhov A V and Zel'dovich B Y 1986 *Mol. Cryst. Liquid Cryst.* **136** 1
[2] Khoo I C 1988 *Prog. Opt.* **26** 107
[3] Santamato E and Shen Y R 1997 *A Guide to Liquid Crystal Research* ed P J Collings and J S Patel (New York: Oxford University Press) ch 14, pp 539–66
[4] Zolot'ko A S, Kitaeva V F, Kroo N, Sobolev N I and Csillag L 1980 *Sov. Phys.–JETP Lett.* **32** 158
[5] Durbin S D, Arakelian S M and Shen Y R 1981 *Phys. Rev. Lett.* **47** 1411
[6] Santamato E, Daino B, Romagnoli M, Settembre M and Shen Y R 1986 *Phys. Rev. Lett.* **57** 2423
[7] Santamato E, Abbate G, Maddalena P, Marrucci L and Shen Y R 1990 *Phys. Rev. Lett.* **64** 1377
[8] Marrucci L, Abbate G, Ferraiuolo S, Maddalena P and Santamato E 1992 *Phys. Rev.* A **46** 4859
[9] Abbate G, Ferraiuolo A, Maddalena P, Marrucci L and Santamato E 1993 *Liquid Cryst.* **14** 1431
[10] Zel'dovich B Y, Merzlikin S K, Pilipetskii N F, Sukhov A V and Tabiryan N V 1983 *Sov. Phys.–JETP Lett.* **37** 676
[11] Zolot'ko A S, Kitaeva V F, Kroo N, Sukhorukov A P, Troshkin V A and Csillag L 1984 *Sov. Phys.–JETP* **60** 488
[12] Cipparrone G, Carbone V, Versace C, Umeton C, Bartolino R and Simoni F 1993 *Phys. Rev.* E **47** 3741
[13] Santamato E, Maddalena P, Marrucci L and Piccirillo B 1998 *Liquid Cryst.* **25** 357
[14] Santamato E, Abbate G, Maddalena P, Marrucci L, Paparo D and Piccirillo B 1999 *Mol. Cryst. Liquid Cryst.* **328** 479
[15] Zolot'ko A S 1981 *Sov. Phys.–JETP* **54** 496
[16] Mauguin C 1911 *Z. Phys.* **12** 1011
[17] Arnone G, Sirleto L, Marrucci L, Maddalena P and Santamato E 1996 *Mol. Cryst. Liquid Cryst.* **282** 191
[18] Marrucci L, Maddalena P, Arnone G, Sirleto L and Santamato E 1998 *Phys. Rev.* E **57** 3033